Variational Models for Cleavage and Shear Fractures

Francesco Freddi[1], Gianni Royer-Carfagni[1]

[1]*Dep. of Civil-Environmental Engineering and Architecture, University of Parma, Italy.*
E-mail: *francesco.freddi@unipr.it, gianni.royer@unipr.it*

SUMMARY.
The fracture pattern in stressed bodies is modeled through the minimization of a regularized functional of the type proposed in [2]. The variational approach is here combined with Structured Deformation Theory to represent that, when the material microstructure is damaged and loosened, particular inelastic (structured) deformations are permitted in the representative volume element. For different-in-type materials (ductile, brittle, quasi-brittle), the structured contribution may vary: by selecting different forms for the admissible class of the structured strain, diverse responses can be captured by the model, such as cleavage, shear, combined cleavage-shear and masonry-like fractures. An energetic competition is engaged between the release of elastic bulk energy and the energy necessary to produce the crack surface. This favors fracture localization.

1 INTRODUCTION

In a fundamental paper [1], Francfort and Marigo first introduced a variational approach to brittle fracture through the minimization of an energy functional, composed of a bulk and a surface energy term à la Griffith, and adding proper irreversibility conditions for crack opening. Later on the same authors, together with Bourdin [2], proposed a variational approximation of this free-discontinuity problem with a *regularized* two field functional, where one field was representative of the macroscopic displacement in the body, while the other one played the role of a damage parameter varying between 0 and 1, with the 0 value in a fractured zone and 1 away from it. This latter formulation leaded to a pseudo spatial-dependent theory since it allows for spatial gradients of the damage parameter to affect the value of the stored energy functional. Extending a result used for the weak formulation of the Munford-Shah functional in problems of image-segmentation [3], it was proved in [2] for the 2-D case that as a characteristic parameter goes to zero, the regularized functional Γ-converges to the Griffith-like functional of [1].

Many deep contributions have been proposed since then and the reader is referred to [4] for an updated survey of the relevant Literature. In general, a *free discontinuity* problem like that of [1] is difficult to solve and therefore one looks for an approximation (usually in the sense of Γ-convergence) through regularized functionals. There are, however, two possible interpretations: the regularized problem may be considered just an useful approximation, or it may be regarded as a damage model *per se*, having its own physical autonomy. This issue has been explain at length in [5], where it has been observed that some parameters introduced in [2] mainly for mathematical purposes are instead important material parameters, with a precise physical significance, that are lost in the limit Griffith-like functional of [1]. In other words, according to this interpretation the regularized functional is *the* model, while its Γ-limit is *the* approximation.

In this paper we take this second point of view and study a pseudo-spatial dependent model in the same category of that of [2], but from a broader viewpoint. In particular, relying upon

Structured Deformations theory by Del Piero and Owen [6], we show that regularized functional of [2] can be extended to reproduce a broader scenario, which accounts for the formation of both mode-I or mode-II fractures, to incorporate various theories of flow and fracture of solids.

In words, when the material is damaged, its microstructure is loosened and because of this, various types of inelastic (structured) deformations become permitted in the representative volume element. According to the material characteristic, the structure part of the deformation may be proportional to the whole strain, and this gives rise to cleavage-like fractures discussed in Section 3.1, or just to the deviatoric part of the strain, producing shear-like (mode II) fractures (see Section 3.2). In all these cases, an energetic competition is engaged between the release of elastic bulk energy and the energy necessary to produce the crack surface. The resulting model is identical to that proposed in [2] for the case of cleavage-like fractures, and to that of [5] for the case of shear-like fractures. Both models are symmetric under tension and compression, in the sense that by reversing the sign of the external actions the crack pattern does not change, although the sign of the corresponding displacement field changes. In general, material compenetration is not avoided.

To overcome these difficulties, a combination of the two aforementioned models can be introduced, accounting for cleavage-like fractures under tension and shear-like fractures under compression, as presented in Section 3.3. When the extended abstract of this paper was submitted to the AIMETA organizing committee, this model was considered a novelty by the authors but later on, when this contribution was still under review, a paper by Amor Marigo and Maurini [4] was published where this idea had been independently developed, even if from a different viewpoint and with diverse purposes. The main difference with the approach presented here consists in the numerical solving algorithm and in the proposed numerical experiments, that are different from those in [4].

The present paper contains however a further case, original to our knowledge, that we have decided to add after the publication of [4] in order to show how our approach is amenable of broad generalization. This case is not mentioned in the extended abstract published in the congress proceedings, because such abstract had been written before the publication of [4]. The peculiarity of this case is that the structured part of the deformation is prescribed to be a symmetric positive semidefinite tensor. This means that only inelastic dilatations due to micro-crack openings are permitted when the material microstructure loosens. Remarkably, the variational approach allows to directly derive that this case, as discussed in Section 3.4, is consistent with the constitutive equations for a classical masonry-like materials defined in [7], i.e., the stress tensor is negative semi-definite, coaxial and orthogonal to the structured strain. However, in the present approach, a certain mechanical work has to be consumed to open a crack, so that localized rather than smeared fractures are energetically favorable. Material interpenetration at the crack-lips is now avoided by the properties of the structured part of the deformation.

The four cases here presented are discussed and compared in the paradigmatic example of a prismatic solid in plane strain in a uniaxial tension or compression test. This is interesting because, in general, the prism may contemporaneously undergo both cleavage and shear fractures. In any case, the approach is feasible of further specialization. Just changing the form of the class of allowable structured deformation field, various models, interpreting the most various responses, can be obtained directly.

2 THE MODEL

If $\mathcal{D}$, $\mathcal{D} = 2\div3$, is the dimension of the Euclidean space where the problem is set, let $\Omega \in \mathbb{R}^{\mathcal{D}}$ denote the undistorted natural reference configuration of the body $\mathcal{B}$ for which the reference frame

{O, x_1, …, x_D} has been defined by the orthogonal base of unit vectors {$\mathbf{e}_1$, … , $\mathbf{e}_D$}. The mapping $\mathbf{y}(\mathbf{x})$: $\Omega \rightarrow \mathbb{R}^D$ is the deformation so that $\mathbf{u}(\mathbf{x}) = \mathbf{y}(\mathbf{x}) - \mathbf{x}$ is the displacement of $\mathbf{x}$.

2.1 *Structured deformation of damaged continuum*

Under assigned actions the body $\mathcal{B}$ may damage and eventually fracture. The resulting deformation is thus the consequence of two causes: the opening of micro- or macro-cracks (*structured* part of the deformation [6]) and the distortion of the elastically bent lamellae delimited by the crack surfaces (*elastic* part of the deformation). We take a *smeared* view of the phenomenon so that the corresponding strain fields can be considered continuous and regular. Under the hypothesis of small strain, the global strain is the symmetric gradient of the displacement field, i.e., $\nabla^s \mathbf{u} = (\nabla \mathbf{u} + \nabla \mathbf{u}^T)/2$, for which we assume a decomposition of the form

$$\nabla^s \mathbf{u}(\mathbf{x}) = \mathbf{E}_e(\mathbf{x}) + \mathbf{E}_s(\mathbf{x}), \tag{2.1}$$

where $\mathbf{E}_e(\mathbf{x})$ and $\mathbf{E}_s(\mathbf{x})$ denote the elastic and structured part of the strain, respectively. We further assume that an internal state variable $s(\mathbf{x})$: $\Omega \rightarrow [0,1] \subset \mathbb{R}$ is defined that represents a damage parameter that takes the 1 value in a sound zone and the 0 value in a completely damaged (fractured) zone. The significance of s is defined by the relation

$$\mathbf{E}_s(\mathbf{x}) = [1 - s(\mathbf{x})] \mathbf{E}_c(\mathbf{x}), \tag{2.2}$$

where $\mathbf{E}_c(\mathbf{x})$ represents the structured deformation that would develop in a neighborhood of the particle $\mathbf{x}$ if, here, the material was completely damaged ($s(\mathbf{x})= 0$). Obviously, $s = 0$ ($s = 1$) implies $\mathbf{E}_s = \mathbf{E}_c$ ($\mathbf{E}_s = \mathbf{0}$), while s taking an intermediate value between 0 and 1 means that the material is not completely damage and, consequently, cannot attain the whole reserve of structured deformation $\mathbf{E}_c$ that would be available in a completely cracked body.

2.2 *The free energy*

Let l represent the characteristic material length scale, that is associated with the characteristic width of the process-zone band associated with the phenomenon of crack coalescence [8]. Under isothermal evolution the Helmholtz free energy depends upon the displacement field $\mathbf{u}(\mathbf{x})$, the damage field $s(\mathbf{x})$ and the structured deformation field $\mathbf{E}_c(\mathbf{x})$ according to a relationship of the type

$$\Pi_l[\mathbf{u}, s, \mathbf{E}_c] = \int_\Omega \Psi(\nabla^s \mathbf{u}, s, \mathbf{E}_c) d\mathbf{x} + \int_\Omega \Gamma_l(s) d\mathbf{x}, \tag{2.3}$$

where $\Psi[\nabla^s \mathbf{u}, s, \mathbf{E}_c]$ represents the bulk part of the energy, whereas $\Gamma_l(s)$ is the surface part, which is suppose to depend on the damage variable s and on the intrinsic material length scale l [8].

For the reasons explained at length in [5], we take for $\Gamma_l(s)$ the expression

$$\Gamma_l(s) = \frac{\gamma}{2} \left[l|\nabla s|^2 + \frac{(1-s)^2}{l} \right], \tag{2.4}$$

where γ is a parameter representative of the material fracture energy.

The bulk energy is associated with the reversible part of the energy stored in the elastically bent lamellae comprised among the microcracks. If $\mathbb{C}$: Sym$\rightarrow$Sym denotes the elasticity tensor of the sound material, then $\Psi(\nabla^s \mathbf{u}, s, \mathbf{E}_c) = \frac{1}{2} \mathbb{C}[\mathbf{E}_e] \cdot \mathbf{E}_e$, where $\mathbf{E}_e$ is defined from (2.1) and (2.2). Observe that, in general, if a fractured body is conveniently constrained, then the sound portions are sufficient to maintain the various pieces together. More precisely, suppose that in a small

neighborhood $\omega(\mathbf{x}) \subset \Omega$ of $\mathbf{x}$, of the same order of the representative volume element, the body is completely damaged ($s(\mathbf{x}) = 0$). Let $\mathbf{H} = \nabla\mathbf{u}(\mathbf{x})$ and consider the problem in which the boundary $\partial\omega(\mathbf{x})$ of $\omega(\mathbf{x})$ is subjected to the Dirichlet condition $\mathbf{y}(\mathbf{x})=(\mathbf{H} + \mathbf{I})\mathbf{x}$, $\forall\mathbf{x}\in\partial\omega(\mathbf{x})$. Then, for any $\mathbf{E} \equiv \nabla^s\mathbf{u}(\mathbf{x})$, we define the relaxed bulk energy density through the expression

$$\Psi^{**}(\nabla^s\mathbf{u}, 0)\Big|_{\nabla^s\mathbf{u}\equiv\mathbf{E}} = \lim_{A(\omega)\to 0} \inf_{\mathbf{E}_c\in\mathcal{S}} \frac{1}{A(\omega)}\int_\omega \Psi(\mathbf{E}, 0, \mathbf{E}_c)d\mathbf{x} \quad , \tag{2.5}$$

where $A(\omega)$ denotes the measure of ω, whereas $\mathcal{S}$ represents the admissible class of structured deformations, which depends upon the material properties. It should be notice that, provided the problem is well-posed, in general (2.5) uniquely defines the tensor $\mathbf{E}_c = \mathbf{E}_c^{**}$ associated with the local value of the strain $\nabla^s\mathbf{u}(\mathbf{x})$. We emphasize this dependence through the notation $\mathbf{E}_c^{**} = \Theta(\nabla^s\mathbf{u})$, indicating that the function Θ: Sym$\to$Sym associates with the local strain $\nabla^s\mathbf{u}$ the unique minimizer $\mathbf{E}_c^{**}$ of (2.5). One can show that in the case of a linear elastic material, the problem (2.5) is indeed well posed because of the convexity of the stored energy. Then, for the case $s \neq 0$, according to the assumed definition (2.2) of damage, one defines from (2.5) the relaxed bulk energy $\Psi^{**}(\nabla^s\mathbf{u},s) = \Psi(\nabla^s\mathbf{u},s, \Theta(\nabla^s\mathbf{u})$). Therefore, $\Psi^{**}(\nabla^s\mathbf{u},s)$ takes the form

$$\Psi^{**}(\nabla^s\mathbf{u}, s) = \frac{1}{2}\mathbb{C}\Big[\nabla^s\mathbf{u} - (1-s)\,\Theta(\nabla^s\mathbf{u})\Big]\cdot\Big(\nabla^s\mathbf{u} - (1-s)\,\Theta(\nabla^s\mathbf{u})\Big)\cdot \tag{2.6}$$

In conclusion, we consider the relaxed minimization problem defined by

$$\min_{(\mathbf{u},s)\in\mathcal{A}} \Pi_l^{**}(\mathbf{u}, s), \quad \Pi_l^{**}(\mathbf{u}, s) = \int_\Omega \Psi^{**}(\nabla^s\mathbf{u}, s)d\mathbf{x} + \int_\Omega \Gamma_l(s)d\mathbf{x}\cdot \tag{2.7}$$

where $\Pi_l^{**}(\mathbf{u}, s)$ denotes the relaxed bulk energy defined by (2.4) and (2.6), whereas $\mathcal{A}$ represents the class of admissible functions ($\mathbf{u}$,s) defined according to the specific conditions for the fields $\mathbf{u}(\mathbf{x})$ and $s(\mathbf{x})$ on the boundary $\partial\Omega$ of Ω. Further conditions upon the minimization problem similar to those of [2] have to be added in order to consider irreversibility of damage. In a load history when the boundary data vary with the time t, the equilibrium state of the body are found through a sequence of minimization problems of the type (2.7), each one corresponding to a small increment of the boundary data, for which we impose that the value of s can never decrease in time.

3 PARTICULAR CASES

Different in type models can be obtained by considering various forms for the class $\mathcal{S}$ of admissible structured deformation in (2.5). For the sake of briefness, in the following we only report the most important results, referring to further work for a more comprehensive treatment.

3.1 *Cleavage fractures*

The simplest case is that in which the structured part of the deformation is directly proportional to the local value of the strain. This means that if $\mathbf{E} \equiv \nabla^s\mathbf{u}(\mathbf{x})$ represents the local value of the strain, then $\mathbf{E}_c =\eta\ \mathbf{E}$, $\eta\in\mathbb{R}$. The value of η can be found from (2.5) and doing so one finds $\eta = 1$. For this case (2.6) reads

$$\Psi^{**}(\nabla^s\mathbf{u}, s) = \frac{1}{2}\mathbb{C}\Big[\nabla^s\mathbf{u} - (1-s)\nabla^s\mathbf{u}\Big]\cdot\Big(\nabla^s\mathbf{u} - (1-s)\nabla^s\mathbf{u}\Big) = \frac{1}{2}s^2\mathbb{C}[\nabla^s\mathbf{u}]\cdot\nabla^s\mathbf{u}\cdot \tag{3.1}$$

Observe, in passing, that for this case one obtains for $\Pi_l^{**}(\mathbf{u}, s)$ of (2.7) an expression which is

substantially similar to

$$\Pi_l^{BFM}[\mathbf{u},s] = \int_\Omega \frac{1}{2}(s^2+k_l)\mathbb{C}[\nabla^s\mathbf{u}]\cdot\nabla^s\mathbf{u}\,d\mathbf{x} + \frac{\gamma}{2}\int_\Omega\left(l\,|\nabla s|^2 + \frac{(1-s)^2}{l}\right)d\mathbf{x}, \tag{3.2}$$

proposed by Bourdin-Francfort and Marigo [2] as a regularization of the variational formulation of Griffith's theory of [1]. The difference consists in the parameter k_l of (3.2), infinitesimal of higher order than l, which was introduced in [2] for numerical purposes but that is here irrelevant for the comparison. This model is capable to reproduce cleavage fractures, but it is symmetric in tension and compression and consequently, in general, it cannot avoid interpenetration of the crack lips.

3.2 *Shear fractures*

Having set $\mathbf{E} \equiv \nabla^s\mathbf{u}(\mathbf{x})$, let $\mathbf{E}_{dev}$ and $\mathbf{E}_{sph}$ denote the deviatoric and spheric part of $\mathbf{E}$ according to $\mathbf{E}_{sph} = \mathbf{I}\,\mathrm{tr}\mathbf{E}/\mathrm{tr}\mathbf{I}$ and $\mathbf{E}_{dev} = \mathbf{E} - \mathbf{E}_{sph}$. Than assume that $\mathbf{E}_c = \eta\,\mathbf{E}_{dev}$, $\eta\in\mathbb{R}$. From (2.5) one finds again $\eta = 1$. The relaxed bulk energy thus takes the form

$$\begin{aligned}\Psi^{**}(\nabla^s\mathbf{u},s) &= \frac{1}{2}\mathbb{C}\left[\nabla^s\mathbf{u} - (1-s)(\nabla^s\mathbf{u})_{dev}\right]\cdot\left(\nabla^s\mathbf{u} - (1-s)(\nabla^s\mathbf{u})_{dev}\right)\\ &= \frac{1}{2}\mathbb{C}\left[(\nabla^s\mathbf{u})_{sph}\right]\cdot(\nabla^s\mathbf{u})_{sph} + \frac{1}{2}s^2\mathbb{C}\left[(\nabla^s\mathbf{u})_{dev}\right]\cdot(\nabla^s\mathbf{u})_{dev},\end{aligned} \tag{3.3}$$

where $(\nabla^s\mathbf{u})_{sph}$ and $(\nabla^s\mathbf{u})_{dev}$ are the spheric and deviatoric part of $\nabla^s\mathbf{u}$. It is worth noticing that $\Pi_l^{**}(\mathbf{u},s)$ of (2.7) assumes for this case an expression identical (modulo the parameter k_l) to

$$\Pi_l^{LR}[\mathbf{u},s] = \int_\Omega \frac{1}{2}\left\{\mathbb{C}[(\nabla^s\mathbf{u})_{sph}]\cdot(\nabla^s\mathbf{u})_{sph} + (s^2+k_l)\mathbb{C}[(\nabla^s\mathbf{u})_{dev}]\cdot(\nabla^s\mathbf{u})_{dev}\right\}d\mathbf{x} + \frac{\gamma}{2}\int_\Omega\left(l\,|\nabla s|^2 + \frac{(1-s)^2}{l}\right)d\mathbf{x}, \tag{3.4}$$

proposed by Lancioni and Royer in [5] to incorporate the idea of less brittle, "deviatoric-like" fractures. In this case there are mainly mode II fractures, and crack-lips interpenetration is consequently mitigated.

3.3 *Combined cleavage-shear fractures*

The models of Sections 3.1 and 3.2 are symmetric in tension-compression, i.e., by reversing the sign of the boundary data one obtains exactly the same crack pattern. But experiments suggest that material response may be remarkably different in tension or compression. Consequently, one can decide to adopt the cleavage fracture model of (3.1) whenever the hydrostatic part $(\nabla^s\mathbf{u})_{sph}$ of the strain $\nabla^s\mathbf{u}$ is non-negative and the shear fracture model of (3.3) when $(\nabla^s\mathbf{u})_{sph} < 0$. Reasoning as in Sections 3.1 and 3.2, one obtains for $\Psi^{**}(\nabla^s\mathbf{u},s)$ the expression

$$\Psi^{**}(\nabla^s\mathbf{u},s) = \begin{cases} \dfrac{1}{2}s^2\mathbb{C}\left[\nabla^s\mathbf{u}\right]\cdot\nabla^s\mathbf{u}, & \text{if } (\nabla^s\mathbf{u})_{sph} \geq 0, \\[2mm] \dfrac{1}{2}\left\{\mathbb{C}\left[(\nabla^s\mathbf{u})_{sph}\right]\cdot(\nabla^s\mathbf{u})_{sph} + s^2\mathbb{C}\left[(\nabla^s\mathbf{u})_{dev}\right]\cdot(\nabla^s\mathbf{u})_{dev}\right\}, & \text{if } (\nabla^s\mathbf{u})_{sph} < 0. \end{cases} \tag{3.5}$$

For the isotropic-elasticity case, a similar model has been recently obtained independently by Amor-Marigo and Maurini [4], who proposed for the energy the expression

$$\Pi_l^{AMM}[\mathbf{u},s] = \int_\Omega \frac{1}{2}\left\{\kappa_0 \frac{\left(tr^-(\nabla^s\mathbf{u})\right)^2}{2} + (s^2+k_l)\left[\kappa_0 \frac{\left(tr^-(\nabla^s\mathbf{u})\right)^2}{2} + \mu\nabla^s\mathbf{u}\cdot\nabla^s\mathbf{u}\right]\right\} d\mathbf{x}, \qquad (3.6)$$

$$+ \frac{\gamma}{2}\int_\Omega\left(l\,|\nabla s|^2 + \frac{(1-s)^2}{l}\right) d\mathbf{x},$$

where κ_0 and μ are the bulk and shear elastic moduli, while $tr^-(\nabla^s\mathbf{u}) = \min\{tr(\nabla^s\mathbf{u}),0\}$ and $tr^+(\nabla^s\mathbf{u}) = \max\{tr(\nabla^s\mathbf{u}),0\}$.

3.4 *Masonry-like fractures*

Let us denote by Sym^+ and Sym^- the set of all positive semidefinite and negative semidefinite symmetric tensors, respectively. The case at hand is characterized by the choice $\mathcal{S} \equiv Sym^+$ in (2.5). The detailed derivation of the function $\mathbf{E}_c^{**} = \mathbf{\Theta}(\nabla^s\mathbf{u})$ from the minimization problem (2.5) requires more space than that allowed here. Consequently, only the final results are recorded.

If $\mathbf{E} \equiv \nabla^s\mathbf{u}(\mathbf{x})$, having set $\mathbf{T}^{**}:=\mathbb{C}[\mathbf{E}- \mathbf{E}_c^{**}]$, one finds that *i)* $\mathbf{E}_c^{**} \in Sym^+$; *ii)* $\mathbf{T}^{**}\in Sym^-$; *iii)* $\mathbf{E} = \mathbb{C}^{-1}[\mathbf{T}^{**}] + \mathbf{E}_c^{**}$; *iv)* $\mathbf{T}^{**}\cdot \mathbf{E}_c^{**} = 0$. These conditions imply that $\mathbf{T}^{**}$ and $\mathbf{E}_c^{**}$ are coaxial. Moreover, in the case of isotropic elasticity when $\mathbb{C} = 2\mu\mathbb{I} + \lambda\mathbf{I}\otimes\mathbf{I}$, being λ and μ the Lamé's elastic constants, then *v)* also $\mathbf{E}$ is coaxial with $\mathbf{T}^{**}$ and $\mathbf{E}_c^{**}$. If one establish a correspondence between the tensor $\mathbf{T}^{**}$ and the Cauchy stress in completely damaged body ($s = 0$), these conditions coincide with the definition of the constitutive equations for a classical linear elastic masonry like material, established in [7]. For any $\mathbf{E}\in Sym$ the aforementioned equations uniquely define the associated structured strain $\mathbf{E}_c^{**}$.

The relaxed bulk energy density takes the form (2.6). Using the property *iv)*, that is, $\mathbb{C}[\nabla^s\mathbf{u} -\mathbf{\Theta}(\nabla^s\mathbf{u})]\cdot \mathbf{\Theta}(\nabla^s\mathbf{u}) = 0$, one finds that (2.6) can be written in the equivalent forms

$$\Psi^{**}(\nabla^s\mathbf{u},s) = \frac{1}{2}\mathbb{C}\left[\nabla^s\mathbf{u}-\mathbf{\Theta}(\nabla^s\mathbf{u})\right]\cdot\left(\nabla^s\mathbf{u}-\mathbf{\Theta}(\nabla^s\mathbf{u})\right) + s^2\frac{1}{2}\mathbb{C}\left[\mathbf{\Theta}(\nabla^s\mathbf{u})\right]\cdot\mathbf{\Theta}(\nabla^s\mathbf{u}).$$
$$= (1-s^2)\frac{1}{2}\mathbb{C}\left[\nabla^s\mathbf{u}-\mathbf{\Theta}(\nabla^s\mathbf{u})\right]\cdot\left(\nabla^s\mathbf{u}-\mathbf{\Theta}(\nabla^s\mathbf{u})\right) + s^2\frac{1}{2}\mathbb{C}\left[\nabla^s\mathbf{u}\right]\cdot\nabla^s\mathbf{u} \qquad (3.7)$$

The corresponding energy functional $\Pi_l^{**}(\mathbf{u},s)$ results from (2.7). It can also be verified that the Cauchy stress T, which is dual in energy with respect to the strain $\nabla^s\mathbf{u}$, reads

$$\mathbf{T} = (1-s^2)\mathbb{C}[\nabla^s\mathbf{u}-\mathbf{\Theta}(\nabla^s\mathbf{u})] + s^2\mathbb{C}[\nabla^s\mathbf{u}] = \mathbb{C}[\nabla^s\mathbf{u}] - (1-s^2)\mathbb{C}[\mathbf{\Theta}(\nabla^s\mathbf{u})]. \qquad (3.8)$$

Notice that when $s = 1$ one finds the stress in a sound elastic material, whereas when $s = 0$ one obtains the expression for a classical masonry-like material [7]. There are however two major novelties of this model with respect to the classical no-tension theory. First, the surface-energy term (2.4) implies that the opening of fractures (i.e., s passing from 1 to 0) is associated with an energy consumption; second, there may be regions where the material is only partially damaged (s between 0 and 1).

4 NUMERICAL EXPERIMENTS

The potentialities of the various models are illustrated and compared through numerical simulations corresponding to one paradigmatic example: a simple uniaxial traction or compression test of a prismatic specimen. In the following, we assume the body is a linear elastic ($\mathbb{C} = 2\mu\mathbb{I} + \lambda\mathbf{I}\otimes\mathbf{I}$,) isotropic material under plain strain. Consequently, the functional of (2.7) has to be

properly specialized to the 2-D case.

4.1 *The numerical implementation*

The model is numerically implemented following the same line of [2], adding an inequality constraint on the scalar damage field *s* similar to that of [5] to impose crack irreversibility. The adopted numerical scheme is based upon an alternate minimization algorithm which, in short, consists in solving a series of minimization sub-problems on $\boldsymbol{u}$ at fixed *s* and *viceversa* on *s* at fixed $\boldsymbol{u}$ up to convergence. In particular, in the cleavage and shear models of Sections 3.1 and 3.2, the energy functionals are quadratic in $\boldsymbol{u}$ and the elastic sub-problem reduces to the solution of a linear system of equations. On the contrary, for the solution of the combined-cleavage-shear-fractures model of Section 3.3, a quasi Newton algorithm is adopted because of the non-linearity induced by the inequality related to the trace of the spherical part of the strain as *per* (3.5). For the masonry-like fractures model of Section 3.4, a fully Newton algorithm has been developed to obtain the equilibrium at each time step. The minimization on *s* at fixed $\boldsymbol{u}$ is reduced to the solution of an unconstrained quadratic problem coupled with an *a posteriori* projection of the solution on the set of admissible space of *s* to enforce the irreversibility condition of fracture. The models have been implemented in an appositely conceived program based upon the Open Source package deal.II [9].

4.2 *Examples*

Consider the two-dimensional rectangular domain of Figure 1, of sides *d* and *h*, which represents a section of the body at hand in plane strain. The element is loaded by applying a vertical displacement on the upper base Γ_2, thus keeping equal to zero the horizontal component. The lower base Γ_1 is kept fixed while the vertical borders Γ_3 and Γ_4 are unconstrained and stress free. This setup may be representative of a tensile or compressive test with un-lubricated loading platens (perfect adhesion due to friction). Following [5] and [4], in order to avoid underestimation of the surface energy necessary to develop fractures at the constrained boundaries, we set $s = 1$ on Γ_1 and Γ_2. In summary, for this case we assume

$$\begin{cases} \mathbf{u} = \mathbf{0}, \quad s = 1, \quad \text{on } \Gamma_1, \\ \mathbf{u} = t\mathbf{e}_2, \quad \mathbf{u} \cdot \mathbf{e}_1 = 0 \quad s = 1, \quad \text{on } \Gamma_2, \\ \mathbf{T} \cdot \mathbf{n} = \mathbf{0}, \quad \nabla s \cdot \mathbf{n} = 0, \quad \text{on } \Gamma_3 \text{ and } \Gamma_4. \end{cases} \quad (4.1)$$

where $\mathbf{e}_1$ and $\mathbf{e}_2$ are the horizontal and vertical unit vectors respectively, $\mathbf{n}$ is the outward normal to the boundary and *t* is scalar parameter positive in traction and negative in compression.

We consider the case $d = 50$ mm, $h = 100$ mm, with elastic constants $\mu = 12500$ N/mm^2 and $\lambda = 8333$ N/ mm^2 (corresponding to Young's modulus $E = 30000$ N/mm^2 and Poisson's ratio $\nu = 0.2$). Furthermore, the fracture toughness γ has been assumed equal to $\gamma = 10^{-3}$ N/mm and the intrinsic length scale $l = 1$ mm. For what the discretization is concerned, we adopted a structured and homogeneous finite element mesh composed of 80000 quadrilaterals, with in total 3x80601 degrees of freedoms. The size of the element is $5 \cdot 10^{-3}$ *d*, that is 0.25 *l*.

Figures 2-3, summarize the results obtained with the different models under traction ($t > 0$) or compression ($t < 0$). All cases are characterized by the sudden appearance of dominant cracks. In cleavage- and shear-fracture models there is no difference between tension or compression, except the sign of the displacement field.

The cleavage-fracture model of (3.1) is characterized by the appearance of two horizontal cracks (figures 2a and 3a) close to the lower and upper bases; the boundary condition $s = 1$ on Γ_1

and Γ_2 avoids ruptures at the constrained contours. Fractures start at the corners where the stress concentration occurs, progress and eventually meet approximately in the middle of the specimens. Their thickness, i.e., the thickness of the strip where s $\cong$ 0, is of the order of l near the corners, but increases towards the center. Since the model is symmetric in tension and compression, there is no difference between figures 2a (traction) and 3a (compression). Obviously, material compenetration due to crack lips overlapping is not avoided under compression (fig. 3a).
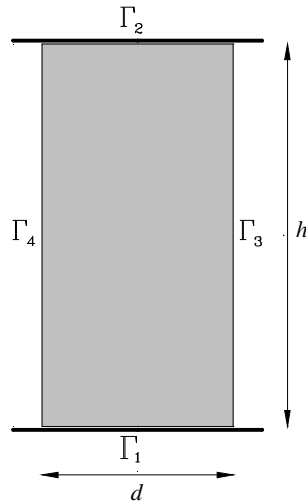
Figure 1: Section of the body in plain strain subjected to uniaxial test.

In the shear-fracture model of (3.3), cracks start again at the specimen corners and propagate towards the center at an angle of approximately $\pi/4$ with respect to the horizontal. The model is again symmetric under traction and compression, presenting equal maps for the damage field. To better illustrate crack propagation, figs. 2b and 3b represent two different stages of the load history that, even though corresponding to tension and compression tests respectively, for the aforementioned symmetry can be considered associated with the same test. At first, two triangular wedges, with bases coinciding with Γ_1 and Γ_2, are isolated (fig. 2b). At this stage, a very small shear stress occurs in the middle of specimen, so that various loading steps are necessary to produce a very slow widening and propagation of cracks through a gently curved shear path, tending to separate the prism into four pieces (fig. 3b). Notice that the model allows only for the slip and not for the opening of crack lips: consequently, the three pieces of fig 2b cannot separate, even if the prism is pulled. Moreover, in general the thickness of shear bands is higher than that of cleavage fractures, a phenomenon outlined in [4] and justified by the high residual stiffness of the model and bad numerical conditioning.

The combined cleavage-shear fractures model of (3.5) presents under traction a crack pattern equal to that of the cleavage model (fig. 2c), but under compression a typical hour-glass failure appears (fig. 3c). The pseudo-vertical fracture in the middle of the specimen is a cleavage fracture provoked by the wedging action of the triangular material portions in proximity of the bases isolated by shear bands, a mechanism not allowed in the shear-fracture model. Notice that also now the thickness of the shear bands is greater than the thickness of the cleavage fracture.

The masonry-like fracture model of (3.7) presents under tension horizontal fractures analogous to that predicted by the cleavage model (fig. 2d). Under compression (Figure 3d), pseudo-vertical fractures occur, which again do not reach the prism's bases Γ_1 and Γ_2, because here the boundary

condition $s = 1$ holds. More in particular, fractures under compression manifest in two successive steps. First, the central vertical fracture appears; second, two new vertical cracks are nucleated symmetrically with respect to the prism axis (fig. 3d). After this, the simulation shows numerical instability. Experiments on quasi-brittle materials like geomaterials or ceramics confirm that cracks appear in a similar way, but failure is due to a second order effect, i.e., the instability of material columns comprised between fractures, that our model cannot reproduce.

| (a) | (b) | (c) | (d) |
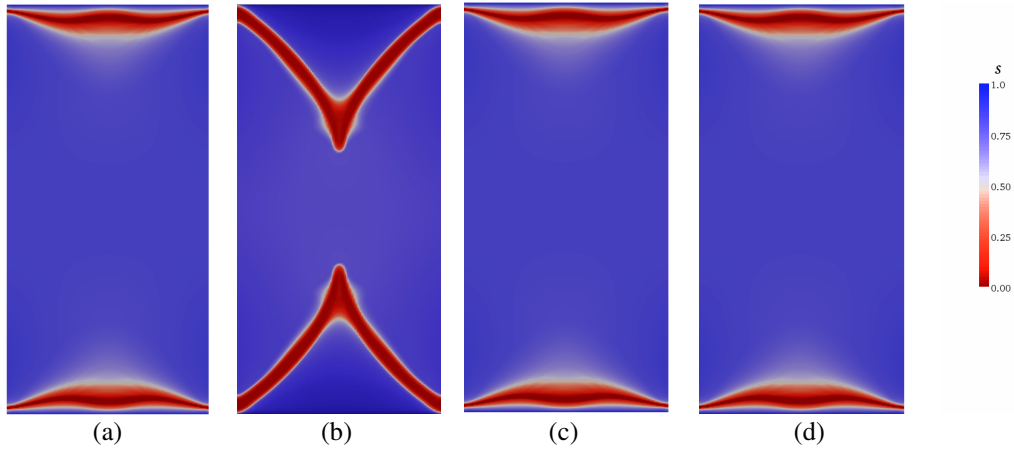
Figure 2: Uniaxial traction test ($t > 0$). Maps of s for different models: a) cleavage fracture; b) shear-fracture at first loading steps; c) combined cleavage-shear fracture; d) masonry-like fracture.

| (a) | (b) | (c) | (d) |
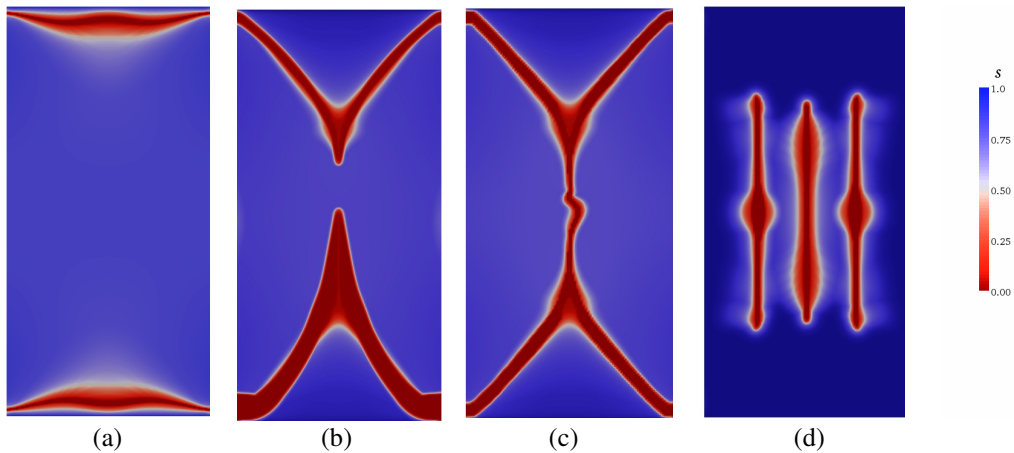
Figure 3: Uniaxial compression test ($t < 0$). Maps of s for different models: a) cleavage fracture; b) shear-fracture at last loading steps; c) combined cleavage-shear fracture; d) masonry-like fracture.

5 CONCLUSIONS

The proposed variational approach to fracture passes through the minimization of a two-field regularized functional that, with respect to other approaches, bypasses the difficulties associated with the discontinuities of the displacement field and the unknown crack location (free

discontinuity problem). Fracture is described by a regular field measuring the damage level in the representative volume element: a crack is not a discontinuity of the displacement field, but a loosening of the microstructure and the corresponding localized weakening of the material rigidity, with the localization of large strains in very narrow bands. The model is minimal since the only required material parameters are the elastic moduli, the fracture surface energy and the material intrinsic length scale. The latter is of particular importance because this formulation is a pseudo spatial-dependent theory and this parameter influences the width of the fracture bands. The gross response of a body may be strain-softening in type due to crack opening but, locally, the material is linear elastic up to fracture: consequently, the numerical implementation results mesh-independent, not suffering the drawbacks of models with strain-softening local constitutive equations.

But the main novelty here is the combination of Structured Deformation Theory within the variational approach. We have showed in paradigmatic examples that just changing the form of the class of admissible functions for the structured strain, very different types of fracture patterns can be obtained. The corresponding micromechanics of cracking may vary between cases usually referred to as cleavage, shear, combined cleavage-shear and masonry-like fractures. However, although some of these classical models (such as the masonry-like solid) take a smeared view of the cracking phenomenon, here the competition between the release of elastic bulk energy and the energy necessary to produce new crack-surface renders fracture localization energetically more favorable than diffuse cracking. Moreover, the form of the structured strain can avoid material interpenetration in the damaged zone. In any case, the potentiality of the proposed approach is yet to be fully explored.

References

[1] Francfort, G. A. and Marigo, J. J., "Revisiting brittle fracture as an energy minimization problem", *J. Mech. Phys. Solids*, **46**, 1319-1342 (1998).
[2] Bourdin, B., Francfort, G. A. and Marigo, J. J., "Numerical experiments in revisited brittle fracture", *J. Mech. Phys. Solids*, **48**, 797-826 (2000).
[3] Ambrosio, L. and Tortorelli, V. M., "Approximation of functional depending on jumps by elliptic functionals via Γ−convergence". *Comm. Pure. Appl. Math.*, **XLIII**, 999-1036 (1990).
[4] Amor, H., Marigo, J.J. and Maurini, C., "Regularized formulation of the variational brittle fracture with unilateral contact: numerical experiments", *J. Mech. Phys. Solids*, **57**, 1209-1229 (2009).
[5] Lancioni, G. and Royer-Carfagni, G., "The variational approach to fracture mechanics. A practical application to the French Panthéon in Paris", *J. of Elasticity*, **95**, 1-30 (2009).
[6] Del Piero, G. and Owen, D.R.,"Structured deformations of continua", *Arch. Rat. Mech. Anal.*, **124**, 99-155 (1993).
[7] Del Piero, G., "Constitutive equations and compatibility of the external loads for linear elastic masonry-like materials", *Meccanica*, **24**, 150-162 (1989).
[8] Bažant, Z. and Planas, S. T., *Fracture and Size-effect in Concrete and other Quasi-Brittle Materials*, CRC press, New York (1998).
[9] Bangerth, W., Hartmann, R., and Kanschat, G., "Deal.II, Differential Equations Analysis Library", *Technical Reference*, http://www.dealii.org, (2009).